

Summer Upwelling in the Northern Continental Shelf of the South China Sea

Z. Y. Jing^{1,2,3}, Z. L. Hua¹, Y. Q. Qi² and H. Zhang³

¹College of Environmental Science and Engineering
Hohai University, Nanjing, 210098 CHINA

²South China Sea Institute of Oceanology
Chinese Academy of Sciences, Guangzhou, 510301 CHINA

³Griffith School of Engineering
Griffith University, Gold Coast, 9726 AUSTRALIA

Abstract

Summer upwelling system in the northern continental shelf of the South China Sea (NCSCS) is investigated with the Pathfinder, Advanced Very High Resolution Radiometer (AVHRR) Sea Surface Temperature (SST), and a three-dimensional, baroclinic, non-linear, numerical model forced by QuikSCAT winds. The AVHRR observation and modelling results have shown the upwelling is a regular phenomenon during summer in the NCSCS. Continental shelf upwelling characteristics are clearly found in the surface and subsurface water, such as low temperature, high salinity and high potential density. They respectively locate in the east of the Hainan Island, the east of the Leizhou Peninsula and the southeast of the Zhanjiang Bay (Qiongdong Upwelling), and the inshore areas from the Shantou Coast to the Nanri Islands of Fujian Coast (Yuedong Upwelling). The centra of the upwelling are mostly located in 111°10'E、19°45'N between the Qinglan Bay and the Qizhou Archipelagoes of eastern Hainan Island, 110°15'E、18°25'N near the Lingshui Bay, 116°45'E、22°50'N of the Shantou Coast and 118°E、23°40'N near the Taiwan Shoal. It is also found that the upwelling areas and centra from modelling results are in agreement with the AVHRR SST.

Key words: Upwelling; the Northern South China Sea; Numerical study; QuikSCAT winds; AVHRR SST

Introduction

The South China Sea (SCS) is a large semi-enclosed tropical marginal sea in the northwest Pacific Ocean with a total area of 3.5 million km² and an average depth of over 2000 m (Figure 1). It is connected with the East China Sea to the northeast, the Pacific Ocean and the Sulu Sea to the east, and the Java Sea and the Indian Ocean to the southwest [1]. Its main body is a broad continental shelf with depth shallower than 200m and isobath parallel to the coastline on the whole [2]. SCS climate is part of the East Asian monsoon system [2, 6]. In this study, seasons always refer to those for the Northern Hemisphere; summer, for example, refers to June, July and August. In winter the SCS is dominated by the strong northeasterly monsoon, whereas in summer the winds reverse the direction to the southwest (Figure 2). From spring to summer, SST in some areas of NCSCS does not increase monotonically with solar radiation, but begins to decrease after the onset of the southwest monsoon, resulting in a pronounced low temperature in summer SST.

The summer upwelling is one of the most outstanding features in the NCSCS (shown in Figure 1) from previous literatures [4-18], such as the description by Wyrтки [6] and Niina & Emery [7]. Upwelling is one of the most important processes in the marine system, because the strong upwelling areas are usually connected with the famous fisheries in the world, such as the Peru upwelling [18], which is the largest fisheries in the world. Many

Chinese large fishery farms are also located in strong upwelling areas of NCSCS. Therefore, it is of great significance to understand the summer upwelling of NCSCS. Based on the Chinese Marine General Survey in 1959~1960, Guan & Cheng [8] have made a preliminary analysis on the summer upwelling of NCSCS. They pointed out that three upwelling areas exist in the coast of NCSCS, which are separately in the east of Hainan Island, Shantou Coast and the east of the Leizhou Peninsula. Moreover, Zeng[9], Yu [10], Han & Ma [11], Han et al. [12], analyzed the local upwellings located in the east of Guangdong coast, Qizhou Archipelagoes, and the east of Hainan Islands respectively according to the different hydrological observational data. Afterwards, Li [4,13] and Hong & Li [5] made further studies to the summer upwelling of NCSCS based on the historical survey data over 20 years, and their results indicated the summer upwelling is a common phenomenon in the NCSCS and the spatial extent of upwelling is a basin-scale in the NCSCS.

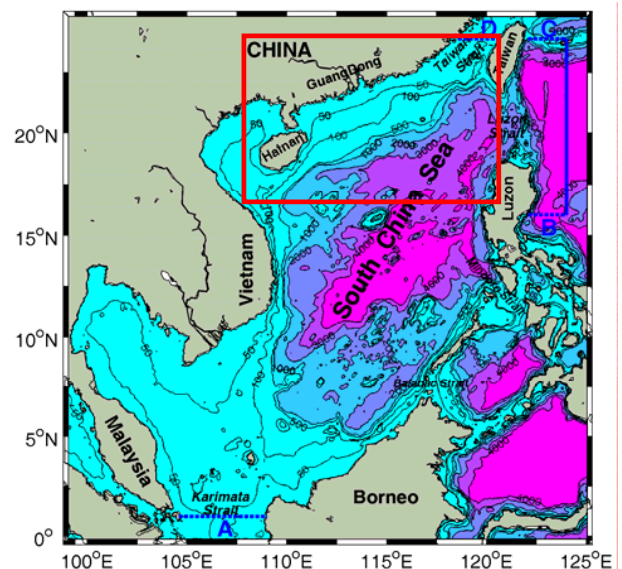


Figure 1. Topography (in meters) of the South China Sea and open boundary locations. Four open boundary positions are respectively located in the A, B, C, D. The area in red rectangle is the NCSCS.

On the other hand, with the prevalent research via numerical modelling and satellite data since the 1980s, many scientists have discussed the SCS summer upwelling and the general circulation, when a primary understanding has been achieved. For example, Guo et al. [15] established a two-dimensional model to study the coastal upwelling according to the survey data between 1959~1990. Zhuang et al. [16] analysed on the SST and wind derived from remote sensing satellite data in the summer of 2000. Their results show that there exist obvious upwelling in the east

of Guangdong coast in summer and the upwelling intensity is closely related to the local wind fields.

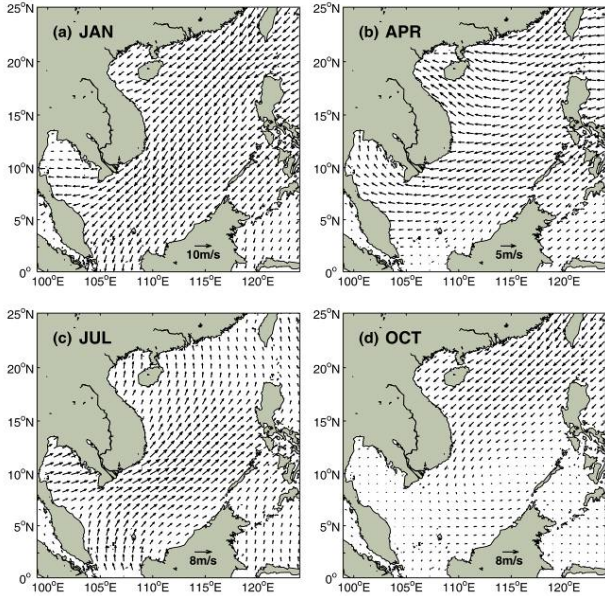


Figure 2. Wind fields derived from QuikSCAT in typical seasons.

However, there were few three-dimensional numerical studies on the summer upwelling in the previous research, and most of the models were usually forced by the monotonous or hypothetical winds. The high spatial and temporal resolution wind data were seldom adopted to simulate the coastal upwelling of NCSCS. In this study, a three-dimensional, baroclinic, non-linear ocean model based on the ECOMSED was used to study the summer upwelling of NCSCS. The model adopted the realistic bottom topography and sea surface heat flux, and especially high spatial and temporal resolution QuikSCAT scatterometer wind data were firstly used in this research, which has been successfully applied to simulate the structure and variation of the southern Benguela upwelling system [17, 18]. At the same time we also consider the main boundary currents of the calculating area such as the Taiwan Warm Current, the Kuroshio and so on. In this study our main aim is to identify and characterize the potential upwelling areas and upwelling centra in the NCSCS by the objective analysis on satellite observation data and the numerical model.

The paper is organized as follows. Firstly, the numerical model and main simulation parameters are introduced. Secondly, the findings of the summer upwelling of NCSCS are discussed, which includes two parts: the AVHRR SST is addressed to provide the essential background and evidence of summer upwelling in the NCSCS; and then the modelling results are discussed regarding upwelling physical characteristics, such as low temperature, high salinity and high density in surface and sublayer water. Some conclusions are given in the end.

Model Approach

Ocean Model

The model ECOMSED is originated from the ECOM (Estuarine, Coastal and Ocean Model) based on the Princeton Ocean Model (POM) by the Blumberg and Mellor [19]. Present version has been developed to a stable and reliable three-dimensional, baroclinic, non-linear, hydrodynamic model, especially reliable for the coastal ocean and estuarine. The main characteristics of ECOMSED are as follows:

- (1) ECOMSED adopts σ -coordinate in the vertical direction, which can accommodate realistic irregular bottom topography;
- (2) The horizontal orthogonal curvilinear coordinate and an "Arakawa C" differencing scheme are used in the ECOMSED, greatly increasing the model efficiency in treating irregularly

coastline and meeting the resolution requirement in the desired regions;

- (3) A second order turbulence closure scheme [20] is imbedded in the model to calculate vertical mixing coefficients; and the horizontal mixing coefficients are parameterized by SMAGORINSKY's scheme [21];

(4) The horizontal time difference is explicit whereas the vertical difference is implicit. The latter eliminates time constraint for the vertical coordinate and can make vertical resolution in the surface and bottom boundary layers come true;

- (5) The model has a free surface and a time-split algorithm. The external model is two-dimensional and uses a short time step based on the CFL condition and the external wave speed. The internal model is three-dimensional and uses a long time step based on the CFL condition and the internal wave speed;

(6) The complete thermodynamics have been implemented in the model;

- (7) ECOMSED also includes the transport modules of suspended sediments, dissolved tracers and neutrally-buoyant particles in estuarine and coastal ocean systems.

Governing Equations

Based on the two simplifying approximations, hydrodynamic assumption that assumed the weight of the fluid identically balances the pressure, and the Boussinesq approximation that assumed density differences are neglected unless the differences are multiplied by gravity, the basic governing equations describe the velocity and surface elevation fields, and the temperature and salinity fields, which form the basis of the circulation model. In the system of horizontal orthogonal curvilinear coordinate and σ -coordinate, $\xi=\xi(x,y)$, $\eta=\eta(x,y)$, $\sigma=(z-\zeta)/(H+\zeta)$, The basic governing equations are as follows.

Continuity Equation:

$$h_1 h_2 \frac{\partial \eta}{\partial t} + \frac{\partial}{\partial \xi_1} (h_2 u D) + \frac{\partial}{\partial \xi_2} (h_1 v D) + h_1 h_2 \frac{\partial w}{\partial \sigma} = 0; \quad (1)$$

Momentum Equation:

$$\begin{aligned} & \frac{\partial (h_1 h_2 Du)}{\partial t} + \frac{\partial}{\partial \xi_1} (h_2 Du^2) + \frac{\partial}{\partial \xi_2} (h_1 Duv) + h_1 h_2 \frac{\partial (wu)}{\partial \sigma} \\ & + Dv \left(-v \frac{\partial h_2}{\partial \xi_1} + u \frac{\partial h_1}{\partial \xi_2} - h_1 h_2 f \right) = -g D h_2 \left(\frac{\partial \eta}{\partial \xi_1} + \frac{\partial H}{\partial \xi_1} \right) \\ & - \frac{g D^2 h_2}{\rho_0} \int_{\sigma}^0 \left(\frac{\partial \rho}{\partial \xi_1} - \frac{\sigma}{D} \frac{\partial D}{\partial \xi_1} \frac{\partial \rho}{\partial \sigma} \right) d\sigma - D \frac{h_2}{\rho_0} \frac{\partial P_a}{\partial \xi_1} + \frac{\partial}{\partial \xi_1} \left(2A_M \frac{h_2}{h_1} D \frac{\partial u}{\partial \xi_1} \right) \\ & + \frac{\partial}{\partial \xi_2} \left(A_M \frac{h_1}{h_2} D \frac{\partial u}{\partial \xi_2} \right) + \frac{\partial}{\partial \xi_2} \left(A_M D \frac{\partial v}{\partial \xi_1} \right) + \frac{h_1 h_2}{D} \frac{\partial}{\partial \sigma} \left(K_M \frac{\partial u}{\partial \sigma} \right), \\ & \frac{\partial (h_1 h_2 Dv)}{\partial t} + \frac{\partial}{\partial \xi_1} (h_2 Duv) + \frac{\partial}{\partial \xi_2} (h_1 Dv^2) + h_1 h_2 \frac{\partial (wv)}{\partial \sigma} \\ & + Du \left(-u \frac{\partial h_1}{\partial \xi_2} + v \frac{\partial h_2}{\partial \xi_1} + h_1 h_2 f \right) = -g D h_1 \left(\frac{\partial \eta}{\partial \xi_2} + \frac{\partial H}{\partial \xi_2} \right) \\ & - \frac{g D^2 h_1}{\rho_0} \int_{\sigma}^0 \left(\frac{\partial \rho}{\partial \xi_2} - \frac{\sigma}{D} \frac{\partial D}{\partial \xi_2} \frac{\partial \rho}{\partial \sigma} \right) d\sigma - D \frac{h_1}{\rho_0} \frac{\partial P_a}{\partial \xi_2} + \frac{\partial}{\partial \xi_2} \left(2A_M \frac{h_1}{h_2} D \frac{\partial v}{\partial \xi_2} \right) \\ & + \frac{\partial}{\partial \xi_1} \left(A_M \frac{h_2}{h_1} D \frac{\partial v}{\partial \xi_1} \right) + \frac{\partial}{\partial \xi_1} \left(A_M D \frac{\partial u}{\partial \xi_2} \right) + \frac{h_1 h_2}{D} \frac{\partial}{\partial \sigma} \left(K_M \frac{\partial v}{\partial \sigma} \right); \end{aligned} \quad (2)$$

Transport Equations of Temperature and Salinity:

$$\begin{aligned} & h_1 h_2 \frac{\partial (D\theta)}{\partial t} + \frac{\partial (h_2 u \theta D)}{\partial \xi_1} + \frac{\partial (h_1 v \theta D)}{\partial \xi_2} + h_1 h_2 \frac{\partial (w\theta)}{\partial \sigma} \\ & = \frac{\partial}{\partial \xi_1} \left(\frac{h_2}{h_1} A_H D \frac{\partial \theta}{\partial \xi_1} \right) + \frac{\partial}{\partial \xi_2} \left(\frac{h_1}{h_2} A_H D \frac{\partial \theta}{\partial \xi_2} \right) + \frac{h_1 h_2}{D} \frac{\partial}{\partial \sigma} \left(K_H \frac{\partial \theta}{\partial \sigma} \right), \\ & \quad (4) \\ & h_1 h_2 \frac{\partial (SD)}{\partial t} + \frac{\partial (h_2 u SD)}{\partial \xi_1} + \frac{\partial (h_1 v SD)}{\partial \xi_2} + h_1 h_2 \frac{\partial (wS)}{\partial \sigma} \\ & = \frac{\partial}{\partial \xi_1} \left(\frac{h_2}{h_1} A_H D \frac{\partial S}{\partial \xi_1} \right) + \frac{\partial}{\partial \xi_2} \left(\frac{h_1}{h_2} A_H D \frac{\partial S}{\partial \xi_2} \right) + \frac{h_1 h_2}{D} \frac{\partial}{\partial \sigma} \left(K_H \frac{\partial S}{\partial \sigma} \right); \end{aligned} \quad (5)$$

State Equation:

$$\rho_{total} = \rho_{total}(\theta, S) \quad (6)$$

Here $D=H+\eta$, η is the water surface elevation and H is the distance from the datum plane to the bottom. Thus the σ ranges from $\sigma=0$ ($z=\eta$) to $\sigma=-1$ ($z=-H$). In the above equations u and v are the velocity components in the ξ_1 and ξ_2 direction respectively. θ is potential temperature, S is salinity; f is the Coriolis parameter; g is the gravitational acceleration. The vertical mixing coefficients K_M and K_H are obtained by a second order turbulence closure scheme [20]. Similarly, the horizontal mixing coefficients A_M and A_H for both momentum and heat/salinity are parameterized by the SMAGORINSKY's scheme [21]. The ρ_0 and ρ respectively represent the reference density and the disturbance density in situ which meet the relation of $\rho_{total} = \rho + \rho_0$.

Parameters and Open Boundary Conditions

The simulation domain in this study is between $99^{\circ}00'E \sim 124^{\circ}00'E$ in longitude and $0^{\circ}00'N \sim 25^{\circ}00'N$ in latitude. The horizontal grid resolution is $10' \times 10'$, and 25 sigma levels are defined in the vertical direction. The baroclinic time-step is 20 min and the barotropic time-step is 30s. In addition, the realistic topography (Figure 1), heat flux, and the boundary currents are adopted in the simulations. At the same time, as the most important factor, the real time QuikSCAT winds derived from the SeaWinds scatterometer are used in the model. The SeaWinds instrument is an active microwave radar designed to measure the electromagnetic backscatter from the wind roughened ocean surface, which was launched on 19 June 1999 onboard the QuikSCAT satellite. The initial temperature and salinity are obtained from WOA01 [3]. The positions of open boundaries set in this study can be found in Figure 1, and the monthly mean throughflows through open boundaries are shown in the Table 1 based on the observation data and the previous research results [6, 22].

Month	Boundaries			
	A	B	C	D
Jan	-3.125	27.375	-23.625	-0.625
Feb	-2.250	29.000	-26.000	-0.750
Mar	-0.750	31.000	-29.000	-1.250
Apr	0.750	32.375	-31.500	-1.625
May	2.250	33.125	-33.500	-1.875
Jun	3.000	32.625	-33.500	-2.125
Jul	3.000	30.875	-31.500	-2.375
Aug	2.125	29.875	-29.625	-2.375
Sep	0.375	29.625	-27.875	-2.125
Oct	-1.250	28.500	-25.500	-1.750
Nov	-2.750	26.500	-22.500	-1.250
Dec	-3.375	26.125	-21.875	-0.875

Table 1. Monthly throughflows through open boundaries ($10^6 \text{ m}^3/\text{s}$)

Simulation Scheme

Firstly, with the climatological monthly mean data (WOA01) as the initial temperature and salinity fields, the model is diagnostically run from January for 12 months driven by climatological winds from the static condition. The diagnostical fields of January mean are obtained as the hotstart conditions for further computation. Then, the model is prognostically run for 5 years, periodically forced by the climatological daily QuikSCAT wind data. The simulation results have illustrated that the total integral kinetic energy has a periodical change. So the simulated 5th year's monthly mean data is used to analyze the upwelling of NCSCS.

Results and Discussion

SST from Satellite Observation

Figure 3 shows the climatological summer AVHRR SST distributions in the NCSCS, which are derived from the Jet Propulsion Laboratory (JPL) of NASA [16]. Low temperature can be observed clearly in both QUA and YUA, mainly located in the east and northeast of the Hainan Island, the east of the Leizhou Peninsula and southeast of the Zhanjiang Bay, and the eastern coast of Guangdong and Fujian, as well as the Taiwan Shoal near the west of the Penghu Archipelagoes. The strong upwellings mainly lie in the coast from southern Sanya to the west of the Qizhou Archipelagoes, where the SST is general $1\sim 2^{\circ}\text{C}$ lower than the offshore SST. Along the Guangdong and Fujian coast the strong upwelling areas are mostly located in the inshore from Hongkong to the Nanri Islands. Particularly along the Shantou and Xiamen Coast large area upwellings occur with a range of $150\sim 200 \text{ km}$ and the SST of $2\sim 3^{\circ}\text{C}$ lower than the offshore SST. Additionally, there is obvious that of the 'crescent moon shape' low temperature band locates in the Taiwan shoal near the west of the Penghu Archipelagoes, where the SST is $2\sim 3^{\circ}\text{C}$ lower than that of the offshore. Therefore it can be found that the summer upwelling in the NCSCS is a regular phenomenon from the analysis of the climatological AVHRR SST, but not a special phenomenon in a specific year as we know before.

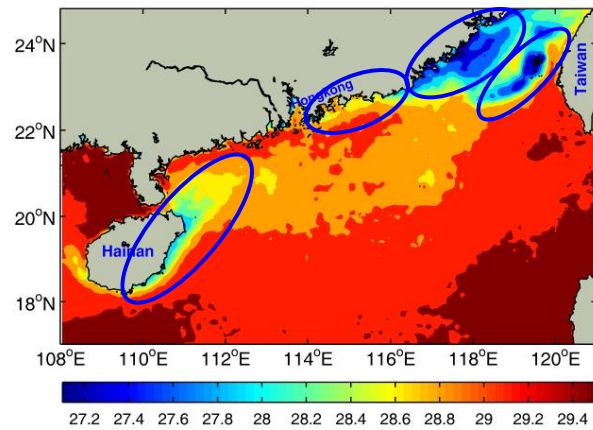


Figure 3. Climatological summer AVHRR SST in the NCSCS.

Modelling Results of Summer Upwelling

Low temperature and high salinity are the typical physical characteristics in the upwelling center. The closed curves composed by low temperature or high isohaline and coastline can be used to confirm the upwelling centre position [9,12]. Figure 4 (a)-(d) show the horizontal distribution of temperature, salinity and density at 5m-layer and 15m-layer. Two strong upwelling areas exist in the NCSCS. One locates in the eastern coast and northeast of the Hainan Island as well as the east of the Leizhou Peninsula and southeast of the Zhanjiang Bay (Qiongdong Upwelling), and the other one is at the Shantou coast and the eastern coast of Guangdong as well as Fujian coast (Yuedong Upwelling) respectively. As in Figure 4 (a)-(d), the typical continental upwelling characteristics, low temperature, high salinity and high potential density are all represented very clearly. The centra of Qiongdong Upwelling mostly lie in $111^{\circ}10'E$, $19^{\circ}45'N$ between the Qinglan Bay and the Qizhou Archipelagoes, and $110^{\circ}15'E$, $18^{\circ}25'N$ near the Lingshui Bay. The Yuedong Upwelling centra are mainly located in $116^{\circ}45'E$, $22^{\circ}50'N$ and $118^{\circ}E$, $23^{\circ}40'N$ near the Shantou Coast and the Taiwan Shoal. The 5m-layer temperature of Qiongdong Upwelling Areas is about 28°C , 1.5°C lower than that of the offshore water at the same latitude, and the 15m-layer temperature is 24°C , 3.5°C lower than that of the offshore and the salinity is 34, 0.2 higher than that of the offshore water. In Yuedong Upwelling Areas, the other strong upwelling area, the

5m-layer center temperature is about 28°C, 1.2~1.5°C lower than that of the offshore water at the same latitude, and the 15m-layer temperature is 25°C, 3~3.5°C lower than that of the offshore water and the salinity is higher than that of the offshore water obviously.

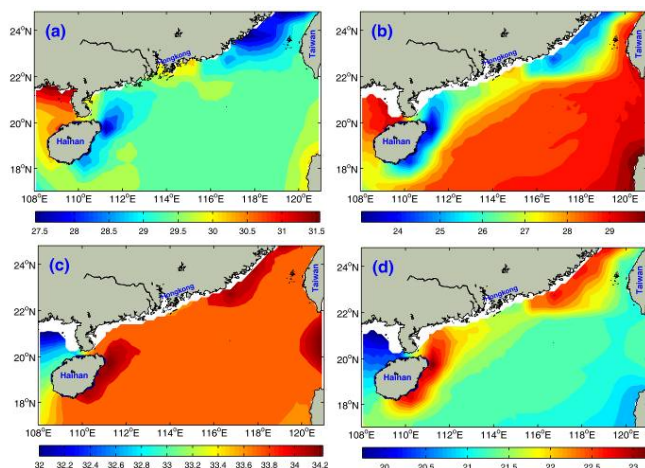


Figure 4. Modelling results of summer upwelling in the NCSCS.

- (a). Temperature of 5m-layer (b). Temperature of 15m-layer
(c). Salinity of 15m-layer (d). Potential density of 15m-layer

Summary and Conclusion

In this study the summer upwelling in the NCSCS is investigated using a three-dimensional, baroclinic, non-linear, prognostic numerical model forced by the QuikSCAT winds. On the other hand satellite remote sensing data are applied to study the summer upwelling of the NCSCS. The modelling results show the typical summer upwelling characteristics in the surface and subsurface water. The upwelling centra shown from modelling results are consistent with the satellite observations. The conclusions obtained from this study are as follows.

- (1) The summer upwelling is a regular phenomenon in the NCSCS. The typical continental shelf upwelling characteristics are clearly shown in the surface and subsurface water, such as low temperature, high salinity and high potential density.
- (2) There are two strong upwelling areas in the NCSCS, QUA and YUA, respectively located in the eastern coast and northeast of the Hainan Island as well as the east of the Leizhou Peninsula and southeast of the Zhanjiang Bay (Qiongdong Upwelling), and the Shantou and the eastern coast of Guangdong as well as the Fujian coast (Yuedong Upwelling).
- (3) The upwelling centra of QUA are mostly located in 111°10'E、19°45'N between the Qinglan Bay and the Qizhou Archipelagoes and 110°15'E、18°25'N near the Lingshui Bay. Those of YUA are mainly located in 116°45'E、22°50'N and 118°E、23°40'N near the Shantou Coast and the Taiwan Shoal.

Acknowledgements

The AVHRR SST is derived from JPL of NASA. The products of QuikSCAT winds data were produced by the IFREMER at the Department of Oceanography from Space (LOS+ CERSAT), and the temperature and salinity are distributed by the Ocean Climate Laboratory (OCL) of National Oceanographic Data Centre (NODC) and the heat flux data were provided by the National Oceanography Centre, Southampton (NOCS).

Literature Cited

- [1] Xie, S.P., Xie, Q., Wang, D.X. & Liu, W.T., Summer upwelling in the South China Sea and its role in regional climate variations, *J. Geophys. Res.*, 108, 2003, 3261-3277.
- [2] Su, J.L., Overview of the South China Sea circulation and its influence on the coastal physical oceanography outside the

Pearl River Estuary, *Continental Shelf Research*, 24, 2004, 1745-1760.

- [3] Hai, J.Y., Liu, Q.Y., Liu Z.Y., Wang, D.X. & Liu, X.B., A general circulation model study of the dynamics of the upper ocean circulation of the South China Sea, *J. Geophys. Res.*, 107, 2002, 3085-4006.
- [4] Li, L., A study on the summer upwellings in shelf waters west to Zhujiang River mouth. *Journal of Oceanography in Taiwan Strait*, 4, 1990, 338-346.
- [5] Hong, Q.M. & Li, L., A study of upwelling over continental shelf off eastern Guangdong. *Journal of Oceanography in Taiwan Strait*, 10, 1991, 272-277.
- [6] Wyrtki, K., Physical oceanography of the Southeast Asia waters, *NAGA Rep.*, 2, 1961, 1-195.
- [7] Niino, H. & Emery, O. Sediment of shallow portions of East China Sea and South China Sea, *Geological Society of American Bulletin*, 72, 1961, 731-761.
- [8] Guan, B.X. & Cheng, S.J., Ocean Current system in East China Sea and South China Sea. Qindao, *Institute of Oceanology, Chinese Academy of Sciences*, 1964.
- [9] Zeng, L.M., A preliminary analysis of indicators of offshore upwelling off eastern Guangdong. *Tropic Oceanology*, 5, 1986, 68-73.
- [10] Yu, W.Q., A preliminary approach of the upwelling for the northern south China Sea. *Marine Science*, 6, 1987, 7-10.
- [11] Han, W.Y. & Ma, K.M., Study of Yuedong Coastal Upwelling. *Acta Oceanologica Sinica*, 10, 1988, 52-59.
- [12] Han, W.Y., Wang, M.B. & Ma, K.B., The lowest surface water temperature area of China sea in summer – the upwelling along the east coast of Hainan Island. *Oceanologia Et Limnologia Sinica*, 21, 1990, 167-275.
- [13] Li L., Summer upwelling system over the northern continental shelf of the South China Sea-physical description., *Proceedings of the Symposium on the Physical and Chemical Oceanography of the China Seas*. Beijing: China Ocean Press, 1993, 58-68.
- [14] Wu, R.S. & Li, L., Summarization of study on upwelling system in the South China Sea, *Journal of Oceanography in Taiwan Strait*, 22, 2003, 269-277.
- [15] Guo, F., Si, M.C. & Xia, Z.W., Two-dimension diagnose model to calculate upwelling on offshore of the east coast of Hainan Island. *Acta Oceanologica Sinica*, 20, 1998, 109-116.
- [16] Zhuang, W., Wang, D.X., Wu, R.S. & Hu, J.Y., Coastal Upwelling off Eastern Fujian-Guangdong Detected by remote Sensing, *Chinese Journal of Atmospheric Sciences*, 29, 2005, 438-444.
- [17] Risien, C.M., Mellor C.J., Reason, C., Shillington, F.A. & Chelton, D.B., Variability in satellite winds over the Benguela upwelling system during 1999-2000. *Journal of Geophysical Research*, 109, 2004, 1-15.
- [18] Bruno, B., Sabrina, S., Abderrahim, B., Claude, R., & Bamol, S., Modelling the structure and variability of the southern Benguela upwelling using QuickSCAT wind forcing. *J. Geophys. Res.*, 110, 2005, 1-18.
- [19] Blumberg A. F. An Estuarine and Coast Ocean Version of POM. *Proceedings of the Princeton Ocean Model Users Meeting*, Princeton, N. J. 1996.
- [20] MELLOR, G.L. & YAMADA, T., Development of a Turbulence Closure Mode Geophysical Fluid Problems, *Reviews of Geophysics and Space Physics*, 20, 1982, 851-875
- [21] Smagorinsky, J., General Circulation Experiments with the Primitive Equations, I. The Basic Experiment. *Monthly Weather Review*, 91, 1963, 99-164.
- [22] Fang, G.H., Zhao, B.R. & Zhu, Y.H., Water volume transport through the Taiwan Strait and the continental shelf of the East China Sea measured with current meters. *Oceanography of Asian Marginal Sea.*, 1991, 345-358.